UCP2 transports C4 metabolites out of mitochondria, regulating glucose and glutamine oxidation

Angelo Vozza[a,1], Giovanni Parisi[a], Francesco De Leonardis[a], Francesco M. Lasorsa[b], Alessandra Castegna[a], Daniela Amorese[a], Raffaele Marmo[a], Valeria M. Calcagnile[a], Luigi Palmieri[a,b,c], Daniel Ricquier[d,e,f], Eleonora Paradies[b], Pasquale Scarcia[a], Ferdinando Palmieri[a,c,2], Frédéric Bouillaud[d,e,f], and Giuseppe Fiermonte[a,c,1,2]

[a]Department of Biosciences, Biotechnologies, and Biopharmaceutics and [c]Center of Excellence in Comparative Genomics, University of Bari, 70125 Bari, Italy; [b]Institute of Biomembranes and Bioenergetics, Consiglio Nazionale delle Ricerche, 70125 Bari, Italy; and [d]Institut National de la Santé et de la Recherche Médicale U1016, Institut Cochin, F-75014 Paris, France; [e]Centre National de la Recherche Scientifique, Unité Mixte de Recherche 8104, 75014 Paris, France; and [f]Université Paris Descartes UMR-S1016, F-75014 Paris, France

Edited* by John E. Walker, Medical Research Council Mitochondrial Biology Unit, Cambridge, United Kingdom, and approved December 2, 2013 (received for review September 16, 2013)

Uncoupling protein 2 (UCP2) is involved in various physiological and pathological processes such as insulin secretion, stem cell differentiation, cancer, and aging. However, its biochemical and physiological function is still under debate. Here we show that UCP2 is a metabolite transporter that regulates substrate oxidation in mitochondria. To shed light on its biochemical role, we first studied the effects of its silencing on the mitochondrial oxidation of glucose and glutamine. Compared with wild-type, UCP2-silenced human hepatocellular carcinoma (HepG2) cells, grown in the presence of glucose, showed a higher inner mitochondrial membrane potential and ATP:ADP ratio associated with a lower lactate release. Opposite results were obtained in the presence of glutamine instead of glucose. UCP2 reconstituted in lipid vesicles catalyzed the exchange of malate, oxaloacetate, and aspartate for phosphate plus a proton from opposite sides of the membrane. The higher levels of citric acid cycle intermediates found in the mitochondria of siUCP2-HepG2 cells compared with those found in wild-type cells in addition to the transport data indicate that, by exporting C4 compounds out of mitochondria, UCP2 limits the oxidation of acetyl-CoA–producing substrates such as glucose and enhances glutaminolysis, preventing the mitochondrial accumulation of C4 metabolites derived from glutamine. Our work reveals a unique regulatory mechanism in cell bioenergetics and provokes a substantial reconsideration of the physiological and pathological functions ascribed to UCP2 based on its purported uncoupling properties.

mitochondrial carrier | glucose and glutamine metabolism | Warburg effect | metabolic reprogramming | diabetes

Mitochondria couple respiratory oxidation of nutrients to ATP synthesis through an electrochemical proton gradient. Proton leak allows partial uncoupling of oxidative phosphorylation, producing heat. Through this mechanism, Uncoupling protein (UCP)1, a member of the mitochondrial carrier family (MCF), regulates adaptive thermogenesis in mammals. In 1997 a protein similar to UCP1 was cloned and named UCP2 (1) based on the assumption that the sequence homology implied a similar function. Whereas UCP1 has a clear-cut uncoupling activity relevant to nonshivering thermogenesis, this is not the case for UCP2. UCP2 has been involved in numerous physiopathological conditions including metabolic disorders, inflammation, ischemic shock, cancer, and aging. Furthermore, changes in UCP2 expression affect metabolic functions (2, 3). It has been suggested that these metabolic actions of UCP2 are due to a mild UCP1-like uncoupling activity (4, 5) that, combined with the generally low levels of UCP2 expression, would regulate the release of reactive oxygen species (ROS) (6) without significantly affecting energy conservation. Although fatty acid-dependent proton transport mediated by UCP2 was reported in reconstituted liposomes (7), a mounting body of evidence argues against UCP2 having an uncoupling activity in vivo (8, 9) and suggests that its central role is in reprogramming metabolic pathways (10). However, the biochemical function of UCP2 has not been disclosed.

Results

Effects of UCP2 Silencing on Glucose Oxidation. We first studied the effects of UCP2 silencing on the mitochondrial oxidation of glucose. Human hepatocarcinoma cells (HepG2) were used as a model because they express high levels of UCP2 (11) and grow efficiently on various carbon sources and their metabolism is well-characterized. UCP2 expression in HepG2 cells was lowered by about 85% by siRNA (Fig. S1 *A* and *B*). As expected from the silencing of an uncoupling protein, the inner mitochondrial membrane potential (Fig. 1*A*) and the ATP:ADP ratio (Fig. 1*B*) were higher in siUCP2-HepG2 cells grown in glucose than in wild-type cells. The effects of UCP2 silencing were much more evident on the energetic charge and the ATP:AMP ratio (Fig. 1*B*), suggesting that UCP2 expression produced an energetic stress. Moreover, siUCP2 cells also contained higher levels of citric acid cycle (CAC) intermediates in the mitochondria (Fig. 1*C*), suggesting that the observed higher ATP:ADP ratio could be mainly due to a more active CAC. These results indicated a lower pyruvate oxidation in wild-type cells, which could be explained by either a reduced glycolytic flux or an impaired

Significance

Mitochondrial carriers constitute a large family of transport proteins that play important roles in the intracellular translocation of metabolites, nucleotides, and coenzymes. Despite considerable research efforts, the biochemical function of Uncoupling protein 2 (UCP2), a member of the mitochondrial carrier family reported to be involved in numerous pathologies, is still elusive. Here we show that UCP2 catalyzes an exchange of malate, oxaloacetate, and aspartate for phosphate, and that it exports C4 metabolites from mitochondria to the cytosol in vivo. Our findings also provide evidence that UCP2 activity limits mitochondrial oxidation of glucose and enhances glutaminolysis. These results provide a unique regulatory mechanism in cell bioenergetics and explain the significance of UCP2 levels in metabolic reprogramming occurring under various physiopathological conditions.

Author contributions: A.V., G.P., L.P., F.P., F.B., and G.F. designed research; G.P., F.D., F.M.L., A.C., D.A., R.M., V.M.C., E.P., and P.S. performed research; A.V., F.M.L., A.C., L.P., F.B., and G.F. analyzed data; and A.V., L.P., D.R., F.P., F.B., and G.F. wrote the paper.

The authors declare no conflict of interest.

*This Direct Submission article had a prearranged editor.

[1]A.V. and G.F. contributed equally to this work.

[2]To whom correspondence may be addressed. E-mail: giuseppe.fiermonte@uniba.it or ferdinando.palmieri@uniba.it.

This article contains supporting information online at www.pnas.org/lookup/suppl/doi:10.1073/pnas.1317400111/-/DCSupplemental.

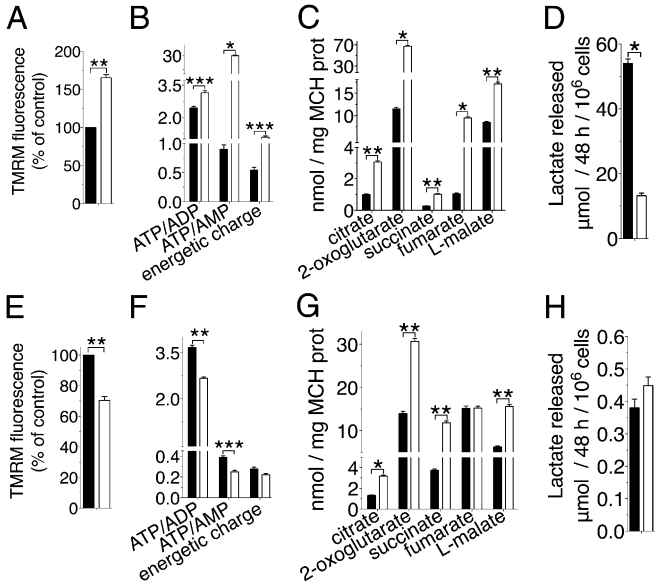

Fig. 1. Effects of UCP2 silencing on glucose and glutamine oxidation. (*A–D*) Glucose-grown cells. (*E–H*) Glutamine-grown cells. Wild-type (black bars) and siUCP2-HepG2 (white bars) cells. (*A* and *E*) Dependence of the mitochondrial membrane potential ($n = 5$). Cell (*B* and *F*) and mitochondrial (MCH) (*C* and *G*) metabolites determined by mass spectrometry are reported ($n = 5$). (*D* and *H*) Lactate released into the medium ($n = 5$). All error bars denote ±SEM (*$P < 0.0006$, **$P < 0.007$, ***$P < 0.04$, *t* test).

CAC. The much higher amount of lactate in the medium released by the wild-type cells (Fig. 1*D*) supported the latter hypothesis, suggesting that most of the ATP found in wild-type cells had a glycolytic origin and that UCP2 limited pyruvate oxidation. UCP2 could accomplish this task by transporting out of mitochondria either pyruvate or, due to its similarity to the mitochondrial dicarboxylate carrier (DIC) (Fig. S2), four-carbon (C4) dicarboxylate CAC intermediates such as oxaloacetate, because the availability of the latter regulates the oxidation of pyruvate-derived acetyl-CoA in mitochondria (12).

Effects of UCP2 Silencing on Glutamine Oxidation. The effects of UCP2 silencing were also studied on glutaminolysis, because glutamine activates the translation of UCP2 (13) and its oxidation in mitochondria does not require oxaloacetate. The membrane potential (Fig. 1*E*) and the ATP:ADP ratio (Fig. 1*F*) were lower in siUCP2-HepG2 cells grown in glutamine than in wild-type cells. These results suggested a reduced oxidative phosphorylation in glutamine-grown siUCP2-HepG2 cells. However, CAC intermediate levels were higher in the mitochondria of siUCP2-HepG2 cells compared with those of wild-type cells (Fig. 1*G*). Furthermore, no significant difference was found in lactate production between the UCP2-silenced and wild-type cells (Fig. 1*H*). All these results are opposite to what would be expected from the silencing of an uncoupling protein, whereas they are consistent with the involvement of UCP2 in the export of C4 metabolites from mitochondria. It is known that glutamine is deamidated to glutamate in mitochondria, which is converted to 2-oxoglutarate either by glutamate dehydrogenase or by aspartate aminotransferase. In many cancer cells, including HepG2, transamination is the major route through which glutamine-derived 2-oxoglutarate enters the CAC (14). The oxidative metabolism of 2-oxoglutarate produces fumarate, malate, and oxaloacetate, which is in equilibrium with aspartate via transamination (15). Malate and aspartate are transported into the cytosol for biosynthetic processes (16). The loss of this efflux would induce the accumulation of C4 metabolites in the mitochondrial matrix, slowing down the last four reversible reactions of the CAC as well as the oxidation of 2-oxoglutarate, which would be diverted toward citrate synthesis through a reductive carboxylation pathway (17). Indeed, the higher level of citrate observed in the cytosol of siUCP2-HepG2 cells (Fig. 2*A*) confirmed the increased mitochondrial synthesis. The lower levels of aspartate (Fig. 2*B*) and malate (Fig. 2*C*) found in the cytosol of siUCP2-HepG2 cells further supported the view that silencing of UCP2 reduced the efflux of C4 metabolites from mitochondria, and the lower levels of glutamate and alanine in the cytosol (Fig. 2*B*) indicated that glutaminolysis was impaired.

UCP2 Catalyzes the Exchange of C4 Metabolites for Phosphate by an H^+-Assisted Mechanism. The putative metabolite transport activity of UCP2 was tested by applying an experimental approach that has been successfully used to characterize many MCF members and is based on the identification of the transported substrates upon reconstitution of the bacterially expressed and purified transporters into liposomes (18). Recombinant UCP2 (Fig. S3*A*) catalyzed a very active uptake of radioactive phosphate (Pi), L-malate, and L-aspartate into proteoliposomes preloaded with the same unlabeled substrate (homo-exchange) (Fig. 3*A*). None of the substrates was transported by recombinant UCP1 to a significant extent (Fig. 3*A* and Fig. S3*B*), which was used as a control. Although the results with UCP1 were expected, the lack of a specific substrate transport activity could also be due to reconstitution of a misfolded protein. Transport of Pi, L-malate, and L-aspartate also occurred unidirectionally, because in the absence of the external counterion a smaller but significant efflux of radioactive substrates from proteoliposomes was observed (Fig. 3*B*, black symbols). In another set of experiments, UCP2 was expressed in *Saccharomyces cerevisiae* lacking the endogenous mitochondrial Pi/H^+ symporter (Mir1p). Homo-exchange experiments with yeast mitochondrial proteins reconstituted into liposomes confirmed the Pi transport activity by either Mir1p or UCP2 (Fig. 3*C*). Similarly, experiments of osmotic swelling with isolated yeast mitochondria in ammonium phosphate demonstrated that the occurrence of an inward H^+-coupled Pi transport depended on the presence of either endogenous Mir1p or recombinant UCP2 (Fig. 3*D*). When swelling experiments were carried out in ammonium malate, the presence of UCP2 did not lead to swelling (Fig. 3*D*), showing that UCP2 does not catalyze a malate/H^+ symport. These conclusions were confirmed using liposomes reconstituted with recombinant UCP2. In these experiments, the protonophore carbonyl cyanide *p*-trifluoromethoxyphenylhydrazone (FCCP), dissipating the pH gradient due to the Pi/H^+ symport, increased

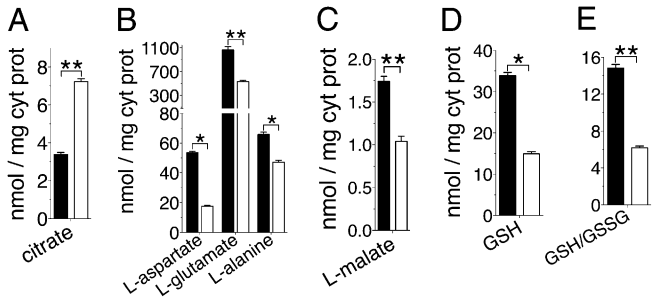

Fig. 2. Cytosolic metabolite levels in siUCP2-HepG2 and wild-type cells grown in the presence of glutamine. Wild-type (black bars) and siUCP2-HepG2 (white bars) cytosolic levels of citrate (*A*), L-aspartate, L-glutamate and L-alanine (*B*), L-malate (*C*) and reduced glutathione (*D*), and the cytosolic ratios between reduced and oxidized glutathione (*E*), determined by mass spectrometry, are reported ($n = 5$). All error bars denote ±SEM (*$P < 0.0006$, **$P < 0.007$, *t* test).

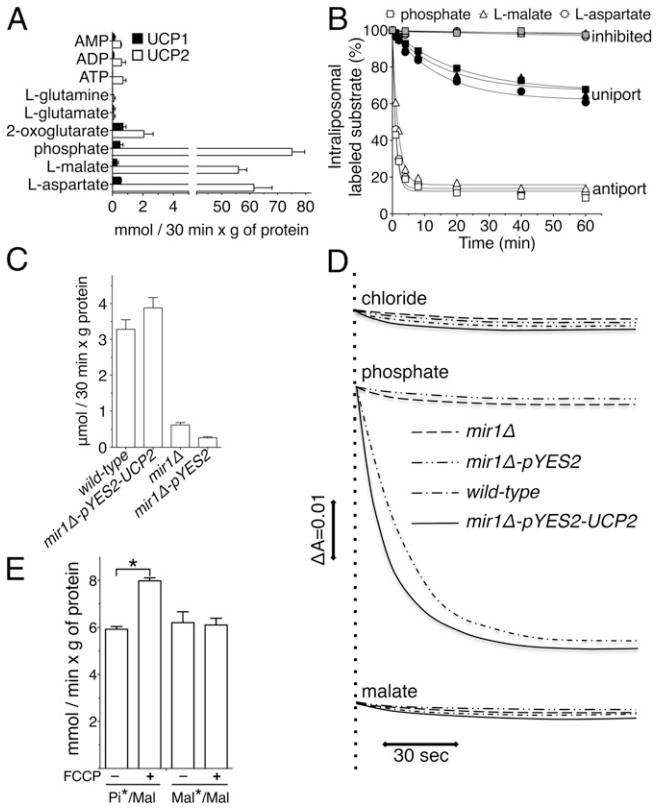

Fig. 3. Functional characterization of transport reactions catalyzed by recombinant UCP2. (*A*) Uptake of radioactive substrates into liposomes reconstituted with recombinant UCP2 and UCP1 and containing the same unlabeled substrate ($n = 3$). (*B*) Efflux of labeled substrates from preloaded proteoliposomes ($n = 3$). (*C*) ^{33}Pi/Pi exchange activity in liposomes reconstituted with yeast mitochondrial extracts ($n = 3$). (*D*) Swelling of yeast mitochondria in isosmotic ammonium solutions of various anions. (*E*) Effect of FCCP on ^{33}Pi/malate and L-[^{14}C]malate/malate exchange reactions in proteoliposomes reconstituted with UCP2. FCCP (5 µM) was added together with the labeled substrate ($n = 5$). All error bars denote ±SEM (*$P < 0.0006$, *t* test).

the rate of the exchange between external Pi and internal malate but had no effect on malate/malate homo-exchange (Fig. 3*E*).

Substrate Specificity of UCP2 Reconstituted into Liposomes. The substrate specificity of UCP2 was assayed by measuring the uptake of ^{33}Pi into proteoliposomes preloaded with various compounds. UCP2 showed a rather narrow specificity, confined to malate, oxaloacetate, aspartate, malonate, sulfate, and phosphate (Fig. 4*A*). This substrate specificity partly overlapped that of the mitochondrial DIC (19), consistent with their relatively close sequence similarity (Fig. S2). However, no other mitochondrial transporter is known to catalyze the aspartate/Pi exchange reaction (18), as was confirmed by the lack of L-[^{14}C]aspartate/Pi exchange activity in the reconstituted mitochondria of siUCP2-HepG2 cells (Fig. 4*B*). As a control, [^{14}C]ATP/ADP exchange was shown to be equally efficient.

Inhibitor Sensitivity of the Substrate-Specific Transport Activity Catalyzed by UCP2. Subsequently, a search for possible modulators of UCP2 transport was carried out (Fig. 4*C*). The ^{33}Pi/Pi exchange reaction catalyzed by UCP2 was inhibited strongly by pyridoxal-5′-phosphate (PLP), bathophenanthroline (BAT), tannic acid, and bromocresol purple (known inhibitors of several mitochondrial carriers) and by butylmalonate and phenylsuccinate, inhibitors of the DIC (19). Genipin, coenzyme Q, retinoic acid, and laurate, modulators of UCP2 protonophoric activity, had no effect on ^{33}Pi/Pi exchange. A significant inhibition was found with GDP and long-chain alkylsulfonates (Fig. 4*C* and Fig. S4 *A*–*C*). Alkylsulfonates and nucleotides inhibit the fatty acid-induced protonophoric activity of UCP2 competitively and not competitively, respectively (20, 21). By contrast, GDP, like malate, oxaloacetate, and aspartate, inhibited the uptake of ^{33}Pi competitively (Fig. S4*B*), with a K_i value of 7.68 ± 0.4 mM. The potency of GDP inhibition of UCP2 substrate transport activity is much less than that previously found of fatty acid-induced protonophoric activity (21, 22). Given its cytosolic level, it is unlikely that GDP can significantly regulate the substrate-specific transport activity of UCP2 in vivo. Long-chain undecanesulfonate acted as a noncompetitive inhibitor (Fig. S4*C*), indicating that its binding to UCP2 is due mainly to its hydrophobic tail, as recently reported for UCP1 (23), with the sulfonate moiety probably interfering with the binding or translocation of UCP2 substrates. Taken together, our findings indicate that UCP2 is a mitochondrial transporter for specific metabolites, like all of the other mitochondrial carriers characterized so far, with the possible exception of UCP1.

Discussion

The metabolomic and transport data presented in this work show that UCP2 catalyzes an exchange of intramitochondrial C4 intermediates for cytosolic phosphate by an H^+-assisted mechanism, which is stimulated in vivo by both the electrical potential (negative inside) and pH gradient (acidic outside) existing across the inner mitochondrial membrane of respiring cells. Our data on the substrate specificity and mechanism of action of UCP2 are consistent with the presence of structural characteristics typical of the carboxylic acid and keto acid class of mitochondrial carriers (24). The identified metabolite transport activity of UCP2 provides a biochemical rationale for the observed metabolic remodeling phenomena associated with the gain or loss of UCP2 function (10, 25). The effects produced by the induction of UCP2 expression in glycolytic cells are summarized in Fig. 5*A*. The mitochondrial concentration of oxaloacetate is usually very

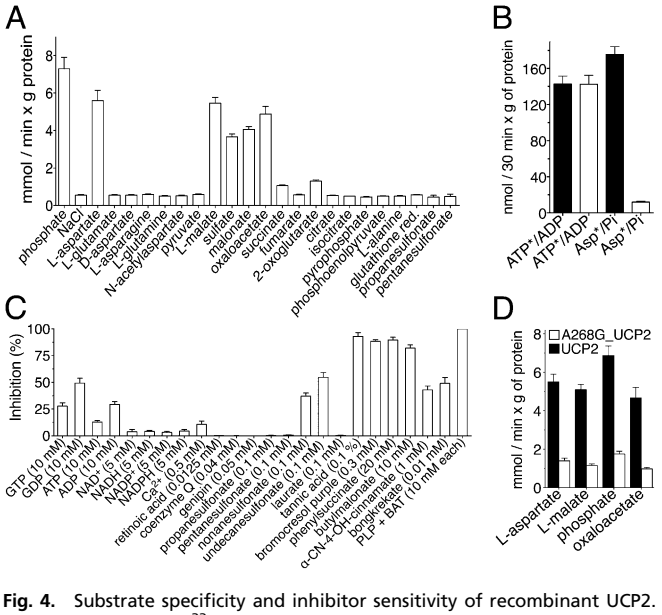

Fig. 4. Substrate specificity and inhibitor sensitivity of recombinant UCP2. (*A*) Uptake of 1 mM ^{33}Pi into UCP2-reconstituted liposomes preloaded internally with various substrates ($n = 4$). (*B*) L-[^{14}C]aspartate/Pi and [^{14}C]ATP/ADP exchanges into liposomes reconstituted with HepG2 (black bars) and siUCP2-HepG2 (white bars) mitochondrial extracts ($n = 3$). (*C*) Inhibition of the ^{33}Pi/Pi exchange reaction in UCP2-reconstituted liposomes by external inhibitors and metabolites ($n = 4$). (*D*) Exchange activities of A268G_UCP2 and UCP2 assayed as in *A* ($n = 4$). All error bars denote ±SEM.

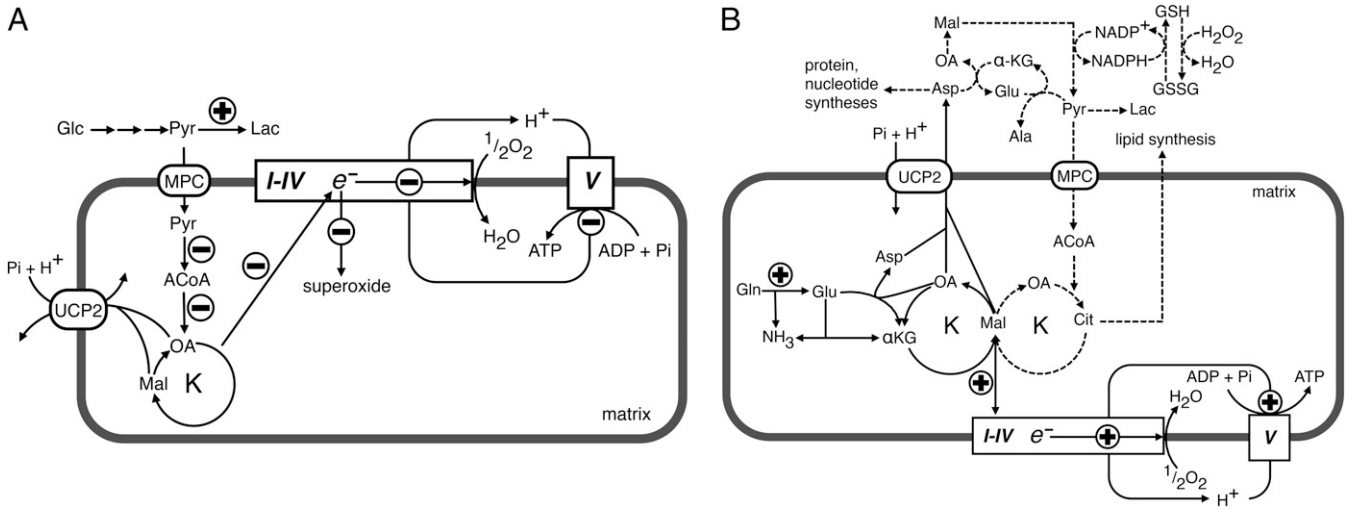

Fig. 5. Influence of UCP2 on mitochondrial activity and metabolism. (*A*) Role of UCP2 in glucose oxidation and (*B*) role of UCP2 in glutamine oxidation. The circled + and – symbols denote the reactions that increased UCP2 activity is expected to accelerate or slow down. Respiratory chain (complexes I–IV) is shown as a rectangle, and ATP synthase (complex V) as a square. ACoA, acetyl-CoA; Ala, alanine; αKG, 2-oxoglutarate; Asp, aspartate; Cit, citrate; Glc, glucose; Gln, glutamine; Glu, glutamate; K, citric acid cycle; Lac, lactate; Mal, malate; MPC, mitochondrial pyruvate carrier; OA, oxaloacetate; Pyr, pyruvate. Dotted lines denote the fate of the glutamine-derived C4 intermediates of the CAC. See text for more explanations.

low, and its availability regulates the entry of acetyl-CoA into the Krebs cycle (12). Therefore, by exporting oxaloacetate and related C4 compounds from mitochondria, UCP2 negatively controls the oxidation of acetyl-CoA–producing substrates via the Krebs cycle, thus lowering the redox pressure on the mitochondrial respiratory chain, the ATP:ADP ratio, and ROS production. Indeed, in quiescent human pluripotent stem cells, high levels of UCP2 expression prevent mitochondrial glucose oxidation, favoring aerobic glycolysis, whereas during cell differentiation, UCP2 is repressed and glucose metabolism is shifted toward mitochondrial oxidation (25). To provide for a less metabolically active CAC, cells consume much more glucose by undertaking aerobic glycolysis. Through this mechanism, UCP2 can mediate the increased glucose utilization in peripheral tissues induced by metformin, the drug of choice for treatment of type 2 diabetes. This drug induces UCP2 expression (26) and produces the same metabolic phenotype (27) that we have observed in wild-type cells (Fig. 1). On the contrary, the induction of UCP2 expression in β-cells has an adverse effect on hyperglycemia, because a reduced ATP:ADP ratio and ROS production together with increased release of lactate would inhibit insulin secretion (28–31). Consistent with this explanation, we have found that replacement of Gly-268 with Ala in UCP2, a mutation associated with congenital hyperinsulinism (32), causes a marked decrease in the transport activity of UCP2 (Fig. 4*D*). The role of UCP2 in glutamine oxidation is illustrated in Fig. 5*B*. Glutamine utilization leads to a net formation of C4 intermediates in the mitochondrial matrix (16), and therefore depends on the continuous export of CAC intermediates and/or aspartate into the cytosol. Our work provides evidence that this task is accomplished by UCP2. The data presented herein are also of interest in cancer research because UCP2 is overexpressed in most cancer cells (33), where it has been shown to have an antiapoptotic function by controlling ROS production (34) and to play a role in the Warburg effect (33, 35). The proliferation of cancer cells requires the rapid synthesis of macromolecules requiring a supply of nucleotides, proteins, and lipids. An increased use of glutamine is required for the success of these synthetic activities to refill the pool of precursor molecules that are generated in the CAC (Fig. 5*B*, dotted lines) (16). The export of C4 compounds from mitochondria mediated by UCP2 is critical for redirecting mitochondrial metabolism toward macromolecular synthesis, and it contributes to the Warburg effect by redirecting glucose utilization from respiration to lactate production (Fig. 5*A*). Based on our findings, UCP2 provides a mechanistic link between enhanced oxidation of glutamine and the Warburg effect, leading to a reduction in both redox pressure on the respiratory chain and production of ROS. Furthermore, recent evidence shows that in pancreatic ductal adenocarcinoma cells, the transport of glutamine-derived aspartate from the matrix to the cytosol is crucial for the maintenance of the cellular redox state by increasing the levels of reduced glutathione (GSH) (36). Notably, UCP2 is overexpressed in pancreatic adenocarcinoma cells (33) and is the only known mitochondrial carrier capable of catalyzing a net efflux of aspartate (in counterexchange for cytosolic phosphate) out of mitochondria, and its silencing in glutamine-grown HepG2 cells reduced the levels of GSH and the GSH:oxidized glutathione (GSSG) ratio (Fig. 2 *D* and *E*).

Through each of these means, UCP2 activity decreases the contribution of glucose to mitochondrial oxidative metabolism and promotes oxidation of alternative substrates such as glutamine and fatty acids. Indeed, Ucp2-KO cells display a metabolic switch from fatty acid oxidation to glucose metabolism (10). Furthermore, UCP2 expression is induced by fasting (37), an observation that led to the questioning of the physiological relevance of its alleged uncoupling activity, as it would increase energy dissipation. Starvation is associated with gluconeogenesis, which requires C4 compounds to be exported from mitochondria, and with ketone body formation, which would benefit from a reduction in the acetyl-CoA acceptor oxaloacetate. The association of UCP2 expression with ketone body formation is well-established (38, 39).

In conclusion, intramitochondrial substrate export catalyzed by UCP2 provides a unique mechanism of bioenergetic control independent of its proposed mild uncoupling activity, which explains the significance of the variation in UCP2 levels in metabolic reprogramming occurring under various physiological and pathological conditions, the diverse tissue distribution of UCP2 in most endotherms, and its presence in the ectotherm kingdom (40).

Materials and Methods

Mammalian Cell Culture. HepG2 and HEK293T cells were grown in DMEM (high glucose) supplemented with 2 and 4 mM glutamine, respectively, 100 U/mL penicillin, 100 μg/mL streptomycin, and 10% (vol/vol) FBS in a humidified, 5% CO_2 incubator at 37 °C. Stable lentivirus transfected clones were grown with puromycin at a concentration of 5 μg/mL. All determinations were carried out on wild-type and UCP2-silenced HepG2 cells grown for 12 h in PBS plus 1.3 mM Ca^{2+}, 50 μM Mg^{2+}, and glucose (5 mM) or glutamine (2 mM).

Generation of Stable UCP2-Silenced Clones. UCP2-silencing oligos were identified using specific algorithms available at http://rnaidesigner.lifetechnologies.com/rnaiexpress/rnaiDesign.jsp; the entire UCP2 mRNA sequence (GenBank, NM_003355.2) was used as a probe. The identified oligos were cloned into the pLKO1 lentiviral vector (Sigma). The constructs were sequenced and used for transfection of HEK293T cells. A detailed description is provided in *SI Materials and Methods*.

Expression Analysis by Real-Time PCR. Total RNA was extracted from HepG2 cells. Real-time PCR was performed in a MicroAmp optical 96-well plate using the automated ABI Prism 7000 sequence detector system (Applied Biosystems). A detailed description is provided in *SI Materials and Methods*.

Dependence of the Mitochondrial Membrane Potential on the Carbon Source. Wild-type and siUCP2-HepG2 cells were grown for 12 h in PBS in the presence of 5 mM glucose or 2 mM glutamine. The membrane potential was measured by fluorescence microscopy using the tetramethylrhodamine methyl ester (TMRM) probe (41). Fluorescent images of treated cells were acquired and fluorescence intensities were analyzed, as previously described (42), through a Zeiss Axiovert 200 microscope equipped with a Photometrics Cascade 512B CCD camera (Roper Scientific) and using MetaFluor software (Universal Imaging).

Lactate Release in Extracellular Medium. One million wild-type and siUCP2-HepG2 cells were grown in 75-cm^2 flasks for 48 h in the presence of 5 mM glucose or 2 mM glutamine; the medium was collected and centrifuged at 700 × *g* for 5 min to remove cell debris. Lactate in the supernatants from both cell types was assayed as described before (43).

Metabolite and Nucleotide Determinations by Mass Spectrometry. For metabolite quantification, cells and cytosolic and mitochondrial fractions were extracted with phenol/chloroform (50/50) and the aqueous phase was centrifuged at 22800 × *g* for 20 min at 4 °C to precipitate the protein fraction. A Quattro Premier mass spectrometer with an Acquity UPLC system (Waters) was used for electrospray ionization LC-MS/MS analysis in the multiple reaction monitoring mode. A detailed description is provided in *SI Materials and Methods*.

Yeast Strains, Growth Conditions, and Swelling of Yeast Mitochondria. BY4742 (wild-type) and *mir1Δ* yeast strains were provided by the EUROFAN resource center EUROSCARF. Mitochondria were isolated by standard procedures. The rate of mitochondrial swelling was monitored by recording the decrease in A_{546} with a Varian spectrophotometer, as previously described (44). A detailed description is provided in *SI Materials and Methods*.

Construction of Expression Plasmids. The coding sequences of UCP2 and UCP1 were amplified from human spleen and fetal cDNAs, respectively. The UCP2 NdeI/HindIII fragment was cloned into the *Escherichia coli* pRUN (45) expression vector and sequenced. The UCP1 BamHI/HindIII fragment was cloned into the *E. coli* pQE30 expression vector (QIAGEN) and sequenced. UCP1 cloning was preceded by site-directed mutagenesis by overlap-extension PCR (46) to remove the BamHI site present in the coding sequence. The A268G mutation was introduced into pRUN-UCP2 (46). The pYES2-UCP2 plasmid was constructed by cloning the human UCP2 coding sequence into the yeast pYES2 expression vector (Invitrogen) under the control of the constitutive *PIC2* promoter. The encoded proteins carried a V5 tag at their C termini.

Bacterial Expression of UCP2, A268G_UCP2, and UCP1. The UCP2 constructs and pQE30-UCP1 were transformed in *E. coli* C0214(DE3) and M15(pREP4) cells, respectively, and protein expression was carried out as previously described (19, 47). Inclusion bodies were purified on a sucrose-density gradient as previously described (48). Control cultures with empty vectors were processed in parallel.

Reconstitution of Recombinant UCP2, A268G_UCP2, and UCP1 into Liposomes and Transport Measurements. UCP2, A268G_UCP2, and UCP1 inclusion bodies were solubilized in 1.6% (wt/vol) *N*-laurylsarcosine. The solubilized proteins were reconstituted by cyclic removal of detergent with a hydrophobic column as described previously (49). Transport was started by adding the labeled substrate. The initial transport rate was calculated from the radioactivity taken up by proteoliposomes after 1 min. The efflux measurements were carried out by adding unlabeled substrates to proteoliposomes containing the labeled substrate. A detailed description is provided in *SI Materials and Methods*.

Other Methods. Proteins were separated by SDS/PAGE and stained with Coomassie blue dye or transferred to nitrocellulose for Western blot analysis. The expression of UCP2 and porin in HepG2 mitochondria was assayed by anti-UCP2 (Santa Cruz Biotechnology) and anti-porin (Sigma-Aldrich) antisera, respectively. A secondary bound peroxidase-conjugated antibody was revealed with the enhanced chemiluminescence reagent kit (ECL; Millipore Immobilon Western).

Statistical Analysis. All statistical analysis was performed using an unpaired two-tailed Student *t* test.

ACKNOWLEDGMENTS. This work was supported by grants from the Ministero dell'Università e della Ricerca (MIUR), the Center of Excellence in Genomics, Apulia Region, and the University of Bari and Italian Human ProteomeNet Grant RBRN07BMCT_009 (MIUR).

1. Fleury C, et al. (1997) Uncoupling protein-2: A novel gene linked to obesity and hyperinsulinemia. *Nat Genet* 15(3):269–272.
2. Andrews ZB (2010) Uncoupling protein-2 and the potential link between metabolism and longevity. *Curr Aging Sci* 3(2):102–112.
3. Diano S, Horvath TL (2012) Mitochondrial uncoupling protein 2 (UCP2) in glucose and lipid metabolism. *Trends Mol Med* 18(1):52–58.
4. Brand MD, Esteves TC (2005) Physiological functions of the mitochondrial uncoupling proteins UCP2 and UCP3. *Cell Metab* 2:85–93.
5. Jaburek M, Garlid KD (2003) Reconstitution of recombinant uncoupling proteins: UCP1, -2, and -3 have similar affinities for ATP and are unaffected by coenzyme Q10. *J Biol Chem* 278(28):25825–25831.
6. Arsenijevic D, et al. (2000) Disruption of the uncoupling protein-2 gene in mice reveals a role in immunity and reactive oxygen species production. *Nat Genet* 26(4):435–439.
7. Jabůrek M, et al. (1999) Transport function and regulation of mitochondrial uncoupling proteins 2 and 3. *J Biol Chem* 274(37):26003–26007.
8. Nedergaard J, Cannon B (2003) The 'novel' 'uncoupling' proteins UCP2 and UCP3: What do they really do? Pros and cons for suggested functions. *Exp Physiol* 88(1):65–84.
9. Stuart JA, Harper JA, Brindle KM, Jekabsons MB, Brand MD (2001) Physiological levels of mammalian uncoupling protein 2 do not uncouple yeast mitochondria. *J Biol Chem* 276(21):18633–18639.
10. Pecqueur C, et al. (2008) Uncoupling protein-2 controls proliferation by promoting fatty acid oxidation and limiting glycolysis-derived pyruvate utilization. *FASEB J* 22(1):9–18.
11. Carretero MV, et al. (1998) Transformed but not normal hepatocytes express UCP2. *FEBS Lett* 439(1-2):55–58.
12. Berry MN (1965) The effects of adenine nucleotides on pyruvate metabolism in rat liver. *Biochem J* 95:587–596.
13. Hurtaud C, Gelly C, Chen Z, Lévi-Meyrueis C, Bouillaud F (2007) Glutamine stimulates translation of uncoupling protein 2mRNA. *Cell Mol Life Sci* 64(14):1853–1860.
14. Cheng T, et al. (2011) Pyruvate carboxylase is required for glutamine-independent growth of tumor cells. *Proc Natl Acad Sci USA* 108(21):8674–8679.
15. Wise DR, et al. (2011) Hypoxia promotes isocitrate dehydrogenase-dependent carboxylation of α-ketoglutarate to citrate to support cell growth and viability. *Proc Natl Acad Sci USA* 108(49):19611–19616.
16. DeBerardinis RJ, et al. (2007) Beyond aerobic glycolysis: Transformed cells can engage in glutamine metabolism that exceeds the requirement for protein and nucleotide synthesis. *Proc Natl Acad Sci USA* 104(49):19345–19350.
17. Mullen AR, et al. (2012) Reductive carboxylation supports growth in tumour cells with defective mitochondria. *Nature* 481(7381):385–388.
18. Palmieri F (2013) The mitochondrial transporter family SLC25: Identification, properties and physiopathology. *Mol Aspects Med* 34(2-3):465–484.
19. Fiermonte G, et al. (1998) The sequence, bacterial expression, and functional reconstitution of the rat mitochondrial dicarboxylate transporter cloned via distant homologs in yeast and *Caenorhabditis elegans*. *J Biol Chem* 273(38):24754–24759.
20. Jezek P, Orosz DE, Modriansky M, Garlid KD (1994) Transport of anions and protons by the mitochondrial uncoupling protein and its regulation by nucleotides and fatty acids. A new look at old hypotheses. *J Biol Chem* 269(42):26184–26190.

21. Zackova M, Skobisová E, Urbánková E, Jezek P (2003) Activating omega-6 polyunsaturated fatty acids and inhibitory purine nucleotides are high affinity ligands for novel mitochondrial uncoupling proteins UCP2 and UCP3. *J Biol Chem* 278(23): 20761–20769.
22. Echtay KS, Winkler E, Frischmuth K, Klingenberg M (2001) Uncoupling proteins 2 and 3 are highly active H(+) transporters and highly nucleotide sensitive when activated by coenzyme Q (ubiquinone). *Proc Natl Acad Sci USA* 98(4):1416–1421.
23. Fedorenko A, Lishko PV, Kirichok Y (2012) Mechanism of fatty-acid-dependent UCP1 uncoupling in brown fat mitochondria. *Cell* 151(2):400–413.
24. Robinson AJ, Overy C, Kunji ERS (2008) The mechanism of transport by mitochondrial carriers based on analysis of symmetry. *Proc Natl Acad Sci USA* 105(46):17766–17771.
25. Zhang J, et al. (2011) UCP2 regulates energy metabolism and differentiation potential of human pluripotent stem cells. *EMBO J* 30(24):4860–4873.
26. Anedda A, Rial E, González-Barroso MM (2008) Metformin induces oxidative stress in white adipocytes and raises uncoupling protein 2 levels. *J Endocrinol* 199(1): 33–40.
27. Zakikhani M, et al. (2012) Alterations in cellular energy metabolism associated with the antiproliferative effects of the ATM inhibitor KU-55933 and with metformin. *PLoS ONE* 7(11):e49513.
28. De Souza CT, et al. (2007) Inhibition of UCP2 expression reverses diet-induced diabetes mellitus by effects on both insulin secretion and action. *FASEB J* 21(4): 1153–1163.
29. Sasaki M, et al. (2013) Reduction of reactive oxygen species ameliorates metabolism-secretion coupling in islets of diabetic GK rats by suppressing lactate overproduction. *Diabetes* 62(6):1996–2003.
30. Pi J, Collins S (2010) Reactive oxygen species and uncoupling protein 2 in pancreatic β-cell function. *Diabetes Obes Metab* 12(Suppl 2):141–148.
31. Brand MD, Parker N, Affourtit C, Mookerjee SA, Azzu V (2010) Mitochondrial uncoupling protein 2 in pancreatic β-cells. *Diabetes Obes Metab* 12(Suppl 2):134–140.
32. González-Barroso MM, et al. (2008) Mutations in UCP2 in congenital hyperinsulinism reveal a role for regulation of insulin secretion. *PLoS ONE* 3(12):e3850.
33. Ayyasamy V, et al. (2011) Cellular model of Warburg effect identifies tumor promoting function of UCP2 in breast cancer and its suppression by genipin. *PLoS ONE* 6(9):e24792.
34. Deng S, et al. (2012) UCP2 inhibits ROS-mediated apoptosis in A549 under hypoxic conditions. *PLoS ONE* 7(1):e30714.
35. Samudio I, Fiegl M, McQueen T, Clise-Dwyer K, Andreeff M (2008) The Warburg effect in leukemia-stroma cocultures is mediated by mitochondrial uncoupling associated with uncoupling protein 2 activation. *Cancer Res* 68(13):5198–5205.
36. Son J, et al. (2013) Glutamine supports pancreatic cancer growth through a KRAS-regulated metabolic pathway. *Nature* 496(7443):101–105.
37. Boss O, et al. (1997) Tissue-dependent upregulation of rat uncoupling protein-2 expression in response to fasting or cold. *FEBS Lett* 412(1):111–114.
38. Nakatani T, Tsuboyama-Kasaoka N, Takahashi M, Miura S, Ezaki O (2002) Mechanism for peroxisome proliferator-activated receptor-alpha activator-induced up-regulation of UCP2 mRNA in rodent hepatocytes. *J Biol Chem* 277(11):9562–9569.
39. Lee SST, et al. (2004) Requirement of PPARalpha in maintaining phospholipid and triacylglycerol homeostasis during energy deprivation. *J Lipid Res* 45(11):2025–2037.
40. Stuart JA, Harper JA, Brindle KM, Brand MD (1999) Uncoupling protein 2 from carp and zebrafish, ectothermic vertebrates. *Biochim Biophys Acta* 1413(1):50–54.
41. Scaduto RC, Jr., Grotyohann LW (1999) Measurement of mitochondrial membrane potential using fluorescent rhodamine derivatives. *Biophys J* 76(1 Pt 1):469–477.
42. Lasorsa FM, et al. (2004) The yeast peroxisomal adenine nucleotide transporter: Characterization of two transport modes and involvement in DeltapH formation across peroxisomal membranes. *Biochem J* 381(Pt 3):581–585.
43. Lindhurst MJ, et al. (2006) Knockout of Slc25a19 causes mitochondrial thiamine pyrophosphate depletion, embryonic lethality, CNS malformations, and anemia. *Proc Natl Acad Sci USA* 103(43):15927–15932.
44. Palmieri F, Klingenberg M (1967) Inhibition of respiration under the control of azide uptake by mitochondria. *Eur J Biochem* 1(4):439–446.
45. Fiermonte G, et al. (2003) The mitochondrial ornithine transporter. Bacterial expression, reconstitution, functional characterization, and tissue distribution of two human isoforms. *J Biol Chem* 278(35):32778–32783.
46. Ho SN, Hunt HD, Horton RM, Pullen JK, Pease LR (1989) Site-directed mutagenesis by overlap extension using the polymerase chain reaction. *Gene* 77(1):51–59.
47. Fiermonte G, et al. (2004) Identification of the mitochondrial ATP-Mg/Pi transporter. Bacterial expression, reconstitution, functional characterization, and tissue distribution. *J Biol Chem* 279(29):30722–30730.
48. Fiermonte G, Walker JE, Palmieri F (1993) Abundant bacterial expression and reconstitution of an intrinsic membrane-transport protein from bovine mitochondria. *Biochem J* 294(Pt 1):293–299.
49. Palmieri F, Indiveri C, Bisaccia F, Iacobazzi V (1995) Mitochondrial metabolite carrier proteins: Purification, reconstitution, and transport studies. *Methods Enzymol* 260: 349–369.